VIP Superconductors Very Important Paper

Deutsche Ausgabe: DOI: 10.1002/ange.201511347
Internationale Ausgabe: DOI: 10.1002/anie.201511347

Structure and Composition of the 200 K-Superconducting Phase of H_2S at Ultrahigh Pressure: The Perovskite $(SH^-)(H_3S^+)$

Elijah E. Gordon[+], Ke Xu[+], Hongjun Xiang, Annette Bussmann-Holder, Reinhard K. Kremer, Arndt Simon, Jürgen Köhler,* and Myung-Hwan Whangbo**

Abstract: *At ultrahigh pressure (> 110 GPa), H_2S is converted into a metallic phase that becomes superconducting with a record T_c of approximately 200 K. It has been proposed that the superconducting phase is body-centered cubic H_3S ($Im\bar{3}m$, $a = 3.089$ Å) resulting from the decomposition reaction $3\,H_2S \rightarrow 2\,H_3S + S$. The analogy between H_2S and H_2O led us to a very different conclusion. The well-known dissociation of water into H_3O^+ and OH^- increases by orders of magnitude under pressure. H_2S is anticipated to behave similarly under pressure, with the dissociation process $2\,H_2S \rightarrow H_3S^+ + SH^-$ leading to the perovskite structure $(SH^-)(H_3S^+)$. This phase consists of corner-sharing SH_6 octahedra with SH^- ions at each A site (the centers of the S_8 cubes). DFT calculations show that the perovskite $(SH^-)(H_3S^+)$ is thermodynamically more stable than the $Im\bar{3}m$ structure of H_3S, and suggest that the A site hydrogen atoms are most likely fluxional even at T_c.*

For H_2S under a pressure of greater than 110 GPa, high-temperature superconductivity has been reported,[1] with a T_c of approximately 200 K. The decomposition of H_2S into H_3S and S under such conditions has been deduced from synchrotron X-ray diffraction (XRD) experiments.[2–4] The obtained XRD patterns can be indexed by considering a mixture of two phases, namely H_3S with a body-centered cubic (bcc) $Im\bar{3}m$ structure and a cell parameter of $a =$ 3.089 Å and sulfur with the β-Po structure.[3,5] Another XRD study under high pressure reported a more complex decomposition mixture that include H_3S and H_4S_3 phases.[6] DFT calculations confirmed the proposed $Im\bar{3}m$ structure of H_3S as the lowest-energy one.[2,7–11]

The $Im\bar{3}m$ structure of H_3S ($a = 3.089$ Å) consists of two interpenetrating SH_3 perovskite sublattices (Figure 1a) with a H···H contact distance of approximately 1.5 Å, which is very short compared with the van der Waals radii sum of 2.4 Å but very long compared with the H–H single-bond length of 0.74 Å in H_2. The decomposition $3\,H_2S \rightarrow 2\,H_3S + S$ implies that the XRD intensities of H_3S and sulfur with the β-Po structure should have a 2:1 ratio. However, a comparison of the simulated XRD patterns with observed ones taken from the literature shows that the amount of sulfur in the samples varies and is always substantially smaller than expected or even hardly detectable (see the Supporting Information, Figure S1). Except for some spurious reflections, the XRD patterns belong to a bcc lattice of sulfur atoms, but do not allow to refine and assign the hydrogen atom positions with

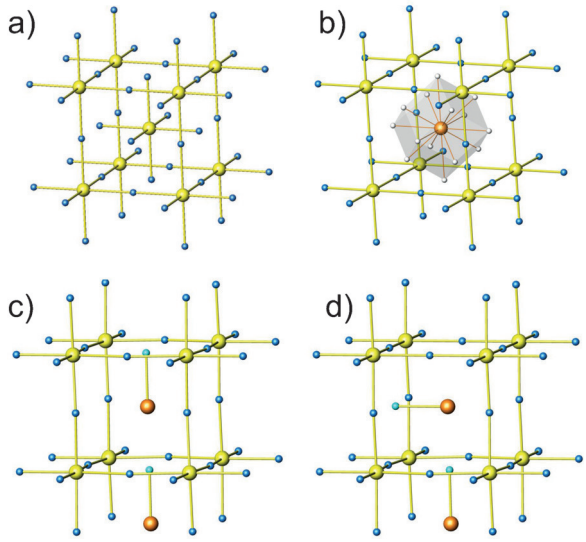

Figure 1. a) The proposed bcc structure of H_3S ($Im\bar{3}m$, $a = 3.089$ Å), emphasizing the presence of two interpenetrating SH_3 perovskite sublattices. b) Structure of the perovskite $(SH^-)(H_3S^+)$ at ultrahigh pressure. The gray polyhedron represents the 14 possible orientations of the S–H bond (8 along the 3-fold rotational axes and 6 along the 4-fold rotational axes). Only one of the 14 positions for the H atom of the SH^- unit is occupied. c) The structure of $(SH^-)(H_3S^+)$ (*P4mm*, SG = 99) with A site S–H bonds pointing to one face of the S_8 cube. d) The structure of $(SH^-)(H_3S^+)$ in which every two adjacent S–H bonds are perpendicular to each other (see text). Large yellow and orange circles correspond to S atoms, and small blue circles to H atoms.

[*] E. E. Gordon,[+] Prof. Dr. M.-H. Whangbo
Department of Chemistry, North Carolina State University
Raleigh, NC 27695-8204 (USA)
E-mail: mike_whangbo@ncsu.edu
K. Xu,[+] Prof. Dr. H. Xiang
Key Laboratory of Computational Physical Sciences (Ministry of Education), State Key Laboratory of Surface Physics, and Department of Physics, Fudan University
Shanghai 200433, P. R. China
K. Xu,[+] Prof. Dr. H. Xiang
Collaborative Innovation Center of Advanced Microstructures, Nanjing 210093, P. R. China
Prof. Dr. A. Bussmann-Holder, Dr. R. K. Kremer, Prof. Dr. A. Simon, Prof. Dr. J. Köhler
Max-Planck-Institut für Festkörperforschung
Heisenbergstrasse 1, 70569 Stuttgart (Germany)
E-mail: j.koehler@fkf.mpg.de
a.simon@fkf.mpg.de
[+] These authors contributed equally.

Supporting information for this article can be found under http://dx.doi.org/10.1002/anie.201511347.

the Rietveld method. The bcc pattern is plotted in red in Figure S1. The diagram in green corresponds to sulfur with the β-Po structure, which should have been formed in the decomposition reaction $3\,H_2S \rightarrow 2\,H_3S + S$; however, sulfur was not observed in the XRD pattern except for one weak reflection at $2\theta = 12°$. Thus the formation of H_3S itself is questionable. The above-mentioned inconsistencies together with the apparent analogies between H_2S and H_2O were our motivation to reinvestigate the structure of the superconducting phase obtained from H_2S at ultrahigh pressure.

Under ambient conditions, H_2O dissociates into H_3O^+ and OH^- to the extent given by $[H_3O^+][OH^-] = 10^{-14}$, which increases by orders of magnitude under high pressure.[2,12] For H_2S, an analogous dissociation process into H_3S^+ and SH^- can be expected to occur under ultrahigh pressure, which would be consistent with earlier ab initio calculations.[13] A perovskite structure $(SH^-)(H_3S^+)$ with the nominal composition H_2S and disordered SH^- units at each A site (the centers of the S_8 cubes) appears to be in reasonable agreement with the observed cubic lattice constant (see Figure 1 b). On the basis of DFT calculations,[14–16] we show herein that the perovskite $(SH^-)(H_3S^+)$ is thermodynamically more favorable than H_3S. In view of the expected dynamic motions of the hydrogen atoms, the functionalities of the S atoms on the A and B sites of the ABO_3 perovskite are expected to interchange easily according to $(SH^-)(H_3S^+) \Leftrightarrow (H_3S^+)(SH^-)$. Furthermore, our calculations reveal that at every A site of the perovskite $(SH^-)(H_3S^+)$, the S–H bonds are preferentially oriented towards any one of the six faces of the S_8 cube (Figures 1 c, d). In case of all A site S–H bonds pointing in one direction, the optimization of the crystal structure of $(SH^-)(H_3S^+)$ results in an arrangement of four H atoms of the H_3S^+ sublattice with short H···H contacts. These H atoms are displaced away from the H atom of the S–H bond (Figure 1 c; for the cif files of this *P*4*mm* structure, see the Supporting Information). Alternatively, neighboring S–H units can be arranged orthogonal to each other (Figure 1 d). There is an infinite number of ways for arranging adjacent S–H bonds with 90° angles. Examples of some planar patterns of orthogonal S–H···S bonds are shown in Figure S2. These pattern have small, but significant energy differences, and the geometry optimization for $(SH^-)(H_3S^+)$ with a staggered pattern of zigzag chains (Figure 2) leads to an *Ima*2 (SG = 46) structure in which H–S bonds with lengths of 1.492 and 1.597 Å alternate. This structure is the most stable one among the optimized structures with the planar patterns shown in Figure S2 (see Table S1 for the cif files of the optimized *Cmmm*, *Cmc*2_1, and *Ima*2 structures). It is important to emphasize that these structure optimizations rely on a static picture whereas in reality, the hydrogen atoms are highly mobile and tunnel from side to side, undergoing a hopping motion through the bcc sulfur lattice. Such a mobile configuration may even lead to plastic-like behavior, which would result in similar conclusions as derived here.[17]

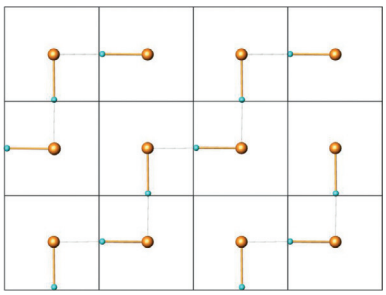

Figure 2. A plane of orthogonally arranged S–H···S bridges made up of the A site S–H bonds forming zigzag chains in $(SH^-)(H_3S^+)$. Hydrogen blue, sulfur orange.

We now estimate the relative stabilities of the H_3S ($Im\bar{3}m$) and $(SH^-)(H_3S^+)$ structures. As the compositions of the two phases are not identical, we first examine the enthalpy change ΔH of the hypothetical reaction:

$$2\,H_3S\ (Im\bar{3}m,\ a = 3.089\ \text{Å}) \rightarrow (SH^-)(H_3S^+) + H_2 \qquad (1)$$

The calculations gave values of $\Delta H = -122.5$, -170.9, and -194.3 meV for the *Cmmm*, *Cmc*2_1, and *Ima*2 structures of $(SH^-)(H_3S^+)$, respectively, confirming that the $(SH^-)(H_3S^+)$ phase is energetically more stable than the H_3S structure ($Im\bar{3}m$). In terms of the free energy, $\Delta G = \Delta H - T\Delta S$, the $(SH^-)(H_3S^+)$ phase is even more favored. As there are three possible orthogonal arrangements of S–H···S bridges at any given A site, fluxional behavior of the A site H atoms as mentioned above will lead to a gain in configuration entropy of $\Delta S = R\ln 3 = 2.18\ \text{cal mol}^{-1}\,\text{deg}^{-1}$. At 200 K, this term contributes $-T\Delta S \approx -18.9$ meV to the free energy, so that the *Cmmm*, *Cmc*2_1, and *Ima*2 structures of $(SH^-)(H_3S^+)$ are more favorable than the H_3S structure ($Im\bar{3}m$) by $\Delta G = -140.4$, -189.8, and -213.2 meV, respectively.

The calculated electronic structure of $(SH^-)(H_3S^+)$ with zigzag chains of S–H bonds (Figure 2) is presented in Figure 3. The occupied S 3p states of the B site sulfur atoms (i.e., the atoms of the perovskite framework) lie lower in energy than the A site sulfur atoms, which dominate the states at the Fermi level. The electronic-structure description of $(SH^-)(H_3S^+)$ is consistent with the formal charges. The flat band observed at the Fermi level along the Γ–X direction

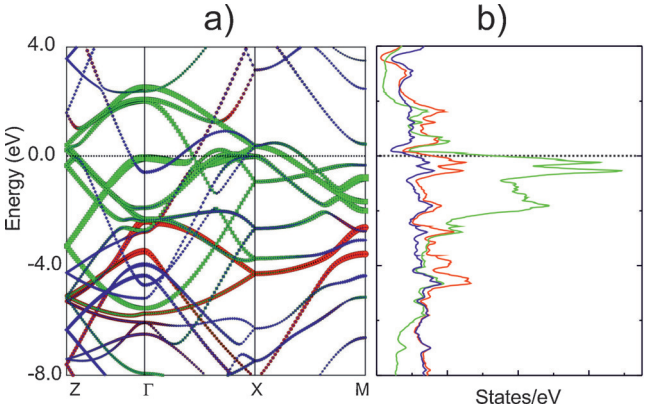

Figure 3. Electronic structure calculated for the ultrahigh-pressure phase of H_2S with the perovskite structure $(SH^-)(H_3S^+)$ and zigzag chains of SH^- units (SG = *Ima*2; see Figure 2). a) Band dispersion relations with fat-band representations; the 3p states of the A site S atoms are shown in green, those of the B site S atoms in red, and the s/p states of the H atoms in blue. b) PDOS plots for the 3p states of the A site S atoms (green), the B site S atoms (red), and the s/p states of the H atoms (blue).

closely resembles the corresponding band structure of the superconductor MgB_2,[18,19] for which multigap superconductivity has been proposed. The Fermi surface exhibits cube-like features (see Figure S3).

The remarkably high T_c values in the range of 80–200 K for the proposed H_3S phase under high pressure have been explained on the basis of the strong-coupling theory of superconductivity,[7,8] with the electron–phonon coupling increasing strongly with an increase in pressure when more than 90% of the coupling arises from H vibrations.[9,10,20,21] This hypothesis is supported by the observation of a substantial isotope effect upon deuteration. However, the T_c value of deuterated D_2S is reduced to approximately 90 K at the highest pressure studied, which corresponds to an isotope exponent of $\alpha \approx 1$; this exponent varies with pressure.[22] Recently, Bianconi and Jahlborg[22] showed that these observations cannot be explained by the single-gap superconductivity theory of Eliashberg[23] and Allen and Dynes,[24] and pointed out the need to consider a multigap superconductivity theory.

In summary, concerning the high-T_c superconducting phase of H_2S formed under high pressure, we have presented a picture that differs from the currently adopted one. In particular, H_2S does not decompose into H_3S and S, but dissociates with the concomitant formation of a perovskite-type structure, $(SH^-)(H_3S^+)$. Furthermore, we suggest that the A site hydrogen atoms are most likely fluxional even at T_c.

Experimental Section

Non-spin-polarized DFT calculations were carried out with the projector-augmented wave method encoded in the Vienna ab initio simulation package[14–16] and the generalized gradient approximation of Perdew, Burke, and Ernzerhof for the exchange–correlation functionals.[16] A plane-wave cutoff energy of 1200 eV and a threshold of self-consistent-field energy convergence of 10^{-8} eV were used. The Brillouin zone was sampled by a set of $12 \times 12 \times 12$ k points.

Acknowledgements

This research used resources of the National Energy Research Scientific Computing Center, a DOE Office of Science User Facility supported by the Office of Science of the U.S. Department of Energy (DE-AC02-05CH11231). H.J.X. thanks the NSFC and the Special Funds for Major State Basic Research.

Keywords: electronic structure · high-pressure chemistry · hydrogen sulfide · perovskite phases · superconductors

How to cite: *Angew. Chem. Int. Ed.* **2016**, *55*, 3682–3684
Angew. Chem. **2016**, *128*, 3746–3748

[1] A. P. Drozdov, M. I. Eremets, I. A. Troyan, V. Ksenofontov, S. I. Shylin, *Nature* **2015**, *525*, 73.
[2] N. Bernstein, C. S. Hellberg, M. D. Johannes, I. I. Mazin, M. J. Mehl, *Phys. Rev. B* **2015**, *91*, 060511.
[3] M. Einaga, M. Sakata, T. Ishikawa, K. Shimizu, M. I. Eremets, A. P. Drozdov, I. A. Troyan, N. Hirao, Y. Ohishi, arXiv: 1509.03156v1.
[4] A. F. Goncharov, N. Goldman, L. E. Fried, J. C. Crowhurst, I.-F. W. Kuo, C. J. Mundy, J. M. Zaug, *Phys. Rev. Lett.* **2005**, *94*, 125508.
[5] D. Duan, X. Huang, F. Tian, D. Li, H. Yu, X. Liu, Y. Ma, B. Liu, W. Tian, T. Cui, *Phys. Rev. B* **2015**, *91*, 180502.
[6] Y. Liu, L. Wang, H. Liu, Y. Zhang, J. Hao, C. J. Pickard, J. R. Nelson, R. J. Needs, W. Li, Y. Huang, I. Errea, M. Calandra, F. Mauri, Y. Ma, *Phys. Rev. B* **2016**, *93*, 020301.
[7] D. Duan, Y. Liu, F. Tian, D. Li, X. Huang, Z. Zhao, H. Yu, B. Liu, W. Tian, T. Cui, *Sci. Rep.* **2014**, *4*, 6968.
[8] D. A. Papaconstantopoulos, B. M. Klein, M. J. Mehl, W. E. Pickett, *Phys. Rev. B* **2015**, *91*, 184511.
[9] I. Errea, M. Calandra, C. J. Pickard, J. Nelson, R. J. Needs, Y. Li, H. Liu, Y. Zhang, Y. Ma, F. Mauri, *Phys. Rev. Lett.* **2015**, *114*, 157004.
[10] R. Akashi, M. Kawamura, S. Tsuneyuki, Y. Nomura, R. Arita, *Phys. Rev. B* **2015**, *91*, 224513.
[11] J. A. Flores-Livas, A. Sanna, E. K. U. Gross, arXiv: 1501.06336v1.
[12] W. L. Marshall, E. U. Franck, *J. Phys. Chem. Ref. Data* **1981**, *10*, 295.
[13] R. Rousseau, M. Boero, M. Bernasconi, M. Parrinello, K. Terakura, *Phys. Rev. Lett.* **2000**, *77*, 1254.
[14] G. Kresse, J. Furthmüller, *Comput. Mater. Sci.* **1996**, *6*, 15.
[15] G. Kresse, J. Furthmüller, *J. Phys. Rev. B* **1996**, *54*, 11169.
[16] J. P. Perdew, S. Burke, M. Ernzerhof, *Phys. Rev. Lett.* **1996**, *77*, 3865.
[17] M. Tachikawa, M. Shiga, *J. Chem. Phys.* **2004**, *121*, 5985.
[18] S. Deng, A. Simon, J. Köhler, *J. Supercond.* **2003**, *16*, 477.
[19] a) S. Deng, A. Simon, J. Köhler, *J. Supercond.* **2004**, *17*, 227; b) S. Deng, A. Simon, J. Köhler, *Int. J. Mod. Phys. B* **2005**, *19*, 29.
[20] E. J. Nicol, J. P. Carbotte, *Phys. Rev. B* **2015**, *91*, 220507.
[21] A. Bianconi, T. Jarlborg, *Europhys. Lett. J.* **2015**, *112*, 37001.
[22] A. Bianconi, T. Jahlborg, *Novel Supercond. Mater.* **2015**, *1*, 37.
[23] a) G. M. Eliashberg, *Sov. Phys. JETP* **1960**, *11*, 696; b) G. M. Eliashberg, *Sov. Phys. JETP* **1961**, *12*, 1000.
[24] P. B. Allen, R. C. Dynes, *Phys. Rev. B* **1975**, *12*, 905.

Received: December 7, 2015
Revised: January 25, 2016
Published online: February 8, 2016

